RESEARCH ARTICLE

Low FOXA2 Expression Is Associated With ECM Remodeling, FAK–YAP-Related Transcriptional Features, and a Macrophage-Enriched Immune-Stromal Microenvironment in Hepatocellular Carcinoma

Zhanwei Wang[1,*], **Siming Xue**[1], **Yuxing Li**[1] **and Judi Zhou**[1]

[1] School of Medicine, Sichuan University, Chengdu 610041, China

Abstract

Tumor-associated macrophages and extracellular matrix remodeling are important components shaping the microenvironment of hepatocellular carcinoma (HCC). This study examined whether forkhead box A2 (FOXA2) expression is associated with extracellular matrix (ECM)/stromal remodeling, focal adhesion kinase (FAK)–Yes-associated protein (YAP)-related transcriptional features, and immune-stromal characteristics in HCC. Using The Cancer Genome Atlas liver hepatocellular carcinoma (TCGA-LIHC) cohort for discovery and the ICGC-LIRI-JP and GSE14520 datasets for expression validation, we performed differential expression, enrichment analysis, single-sample gene set scoring, ESTIMATE-based microenvironment assessment, and Cox regression, with FOXA2-high and FOXA2-low groups defined by the cohort-specific median. FOXA2 expression was consistently reduced in HCC tissues and associated with unfavorable overall survival (log-rank $P = 0.006$). FOXA2-low tumors showed higher ECM/stromal remodeling and FAK–YAP-related scores, enrichment of fibroblast, M2 macrophage, regulatory T-cell, endothelial, and immune checkpoint-related signatures, and decreased CD8-positive T-cell and M1 macrophage signatures; exploratory enrichment also indicated altered lipid metabolism-related programs. These co-occurring bulk features do not establish a causal FOXA2–ECM–FAK–YAP–immune pathway. Low FOXA2 expression therefore marks an HCC transcriptional state characterized by stromal remodeling, mechanotransduction-related features, and immunosuppressive signatures. Single-cell, spatial, protein-level, and functional validation is required to determine the underlying cellular origin and mechanism.

Keywords: Hepatocellular carcinoma, FOXA2, extracellular matrix, mechanotransduction, tumor microenvironment.

Submitted: 29 July 2026
Revised: 17 September 2026
Accepted: 19 September 2026
Published: 24 September 2026

Vol. 1, **No.** 2, 2026.
10.62762/OC.2026.549981

***Corresponding author:**
Zhanwei Wang
984880035@qq.com

Citation
Wang, Z., Xue, S., Li, Y., & Zhou, J. (2026). Low FOXA2 Expression Is Associated With ECM Remodeling, FAK–YAP-Related Transcriptional Features, and a Macrophage-Enriched Immune-Stromal Microenvironment in Hepatocellular Carcinoma. *Oncology Communications*, 1(2), 95–107.

© 2026 by the Authors. Published by Institute of Central Computation and Knowledge. This is an open access article under the CC BY license (https://creativecommons.org/licenses/by/4.0/).

1 Introduction

Hepatocellular carcinoma (HCC) is the most common pathological type of primary liver cancer and poses a major global health burden. Although surgical resection, liver transplantation, locoregional therapy, targeted therapy, and immune checkpoint blockade have improved clinical outcomes in selected patients, the prognosis remains unsatisfactory for patients with advanced or recurrent disease. HCC usually arises against a background of chronic hepatitis, fibrosis, or cirrhosis, indicating that tumor-intrinsic alterations and the surrounding liver microenvironment jointly drive disease progression. Identifying molecular features associated with both tumor differentiation and microenvironmental remodeling may therefore deepen our biological understanding and facilitate prognostic stratification [1].

The tumor microenvironment of HCC consists of malignant hepatocytes, fibroblasts, endothelial cells, immune cells, and extracellular matrix (ECM) components [2]. Excessive deposition and crosslinking of collagen, fibronectin, periostin, and other matrix proteins correlate with fibrosis, impaired cell adhesion, tumor cell migration, epithelial–mesenchymal transition (EMT), and treatment resistance. ECM accumulation and remodeling can lead to increased tissue stiffness and modulate anti-tumor immunity; however, transcriptomic ECM signatures are indirect surrogates and are not direct measurements of mechanical stiffness [3–5].

Mechanotransduction transmits extracellular mechanical cues to intracellular signaling pathways. Integrin-associated focal adhesion kinase (FAK) and the Hippo effectors Yes-associated protein (YAP) and transcriptional coactivator with PDZ-binding motif (TAZ) are core components of this process. Elevated matrix stiffness can induce FAK phosphorylation and YAP nuclear localization, which further triggers TEA domain (TEAD)-dependent transcription of genes including *CTGF* (*CCN2*), *CYR61* (*CCN1*), and *ANKRD1* [6, 7]. Since FAK phosphorylation and YAP localization are predominantly regulated at the protein and subcellular levels, pathway scores derived from gene expression profiles reflect mechanotransduction-related transcriptional states rather than direct biochemical activity.

FOXA2 is a pioneer transcription factor that participates in liver development, hepatocyte differentiation, chromatin accessibility, and metabolic homeostasis [8, 9]. Its biological functions in cancer are context-dependent. In HCC, FOXA2 is associated with differentiation-related molecular programs, tumor progression and treatment response, and it exerts divergent effects under different biological and therapeutic conditions [10]. The correlation between FOXA2 expression and stromal remodeling as well as mechanotransduction-related transcriptional states in bulk HCC datasets has not been fully elucidated.

Previous studies have independently reported ECM remodeling, mechanotransduction, immune-stromal heterogeneity and FOXA2 dysregulation in HCC. Any associations among these features may arise from direct regulatory interactions, altered tumor-cell differentiation, variations in tumor purity, or changes in stromal cell abundance. Transcriptomic analyses can verify the consistency and prognostic relevance of these associations, yet they cannot determine the causal direction or cellular origin of such relationships.

In this study, we analyzed public transcriptomic cohorts of HCC to evaluate FOXA2 expression, clinical outcomes, gene expression associated with ECM/stromal remodeling, FAK–YAP-related transcriptional signatures, and immune-stromal features. The TCGA-LIHC cohort served as the discovery set, and independent datasets were adopted for expression validation when data were compatible. This study was designed for association analysis and cannot confirm direct FOXA2 binding, matrix elasticity, FAK phosphorylation, or YAP nuclear translocation.

2 Materials and Methods

2.1 Study Design

This retrospective computational study assessed the associations among FOXA2 expression, clinical outcomes, ECM/stromal remodeling-related transcriptional features, FAK–YAP-related gene expression, and the inferred tumor microenvironment in HCC. The TCGA-LIHC cohort served as the discovery cohort. The ICGC-LIRI-JP and GSE14520 datasets were adopted for external expression validation and supportive molecular comparisons when compatible annotations were available.

The workflow was composed of five parts: (1) comparison of FOXA2 expression between tumor and non-tumor tissues; (2) evaluation of clinical and survival associations; (3) differential expression and pathway enrichment analyses; (4) calculation of predefined ECM/stromal remodeling and FAK–YAP-related transcriptional scores; and (5)

estimation of tumor purity and immune-stromal signatures. The study was designed to characterize associations among these features, and all mechanistic interpretations were treated as hypothesis-generating.

2.2 Public Transcriptomic Data Collection

RNA-sequencing data and corresponding clinical information were retrieved from the TCGA-LIHC cohort [11]. The TCGA-LIHC expression dataset comprised 374 primary HCC tumor samples and 50 adjacent non-tumor samples. The 374 tumor samples constituted the starting population for tumor-only transcriptomic, signature, correlation, and tumor-microenvironment analyses, whereas analyses requiring survival or clinicopathological annotations were restricted to cases with complete information; 364 cases were available for the median-group survival and clinicopathological analyses reported below. The ICGC-LIRI-JP [12] and GSE14520 [13] datasets were included as external datasets. Only human HCC samples with clear tissue classification and available FOXA2 expression data were used for expression comparisons.

Clinical variables were harmonized whenever possible, including survival time, survival status, tumor stage, histological grade, vascular invasion, age, sex, and serum alpha-fetoprotein (AFP). All analyses were conducted within individual cohorts rather than by directly pooling expression values across RNA-sequencing and microarray platforms. For GSE14520, the available platform and series-matrix annotations were used to identify compatible HCC and non-tumor samples, and expression values were analyzed separately from the RNA-sequencing cohorts.

2.3 Data Preprocessing and Normalization

For TCGA-LIHC, the gene-by-sample expression matrix was analyzed after $\log_2(\text{TPM} + 1)$ transformation (TPM, transcripts per million) for visualization, correlation analysis and single-sample signature scoring. Raw counts were used for count-based differential expression whenever available. Low-expression genes were filtered using the prespecified analysis rule. Microarray probes were mapped to official HUGO Gene Nomenclature Committee (HGNC) gene symbols according to the corresponding platform annotation, and multiple probes mapping to the same gene were aggregated consistently within the dataset.

Quality control procedures included inspection of expression distributions, sample annotations, missing clinical data and principal component patterns. Cross-platform expression values were never pooled directly. Because the cohorts were analyzed separately, no cross-platform batch correction was applied.

2.4 FOXA2 Expression and Clinicopathological Association Analysis

FOXA2 expression was compared between paired tumor and adjacent non-tumor tissues using the paired Wilcoxon signed-rank test, while comparisons between independent groups were performed using the Wilcoxon rank-sum test. Associations between FOXA2 expression and tumor stage, histological grade, vascular invasion and other clinical variables were evaluated only in samples with complete annotations for the variable under study.

FOXA2 expression was treated as a continuous variable in the primary Cox regression framework. For Kaplan–Meier visualization and descriptive comparisons, the TCGA-LIHC analysis cohort was dichotomized at the cohort-specific median FOXA2 expression value into FOXA2-low and FOXA2-high groups ($n = 182$ per group among the 364 cases used for the median-group analyses). Overall survival served as the primary time-to-event endpoint. Multivariable Cox models incorporated available clinical covariates. Because FOXA2 and the transcriptomic signature scores are correlated bulk-expression features, multivariable estimates were interpreted cautiously.

2.5 Differential Expression and FOXA2-Associated Transcriptional States

For descriptive differential expression analysis, tumors from the TCGA-LIHC cohort were stratified at the cohort-specific median FOXA2 expression value. Differential expression was evaluated within the processed TCGA-LIHC expression matrix using FOXA2-low versus FOXA2-high as the principal contrast. Genes with a Benjamini–Hochberg-adjusted P value < 0.05 and an absolute $\log_2$ fold change > 1.0 were retained for reporting.

Functional enrichment analyses covered Gene Ontology (GO) biological processes, Kyoto Encyclopedia of Genes and Genomes (KEGG) pathways and gene set enrichment analysis (GSEA) [14]. Multiple-testing correction was applied to the enrichment analyses. These results were interpreted as transcriptional associations linked to FOXA2 expression states rather than evidence that

FOXA2 directly binds to or regulates the enriched genes.

2.6 ECM/Stromal Remodeling-Related Signature Scoring

An ECM/stromal remodeling-related signature was defined based on the genes *COL1A1*, *COL1A2*, *COL3A1*, *LOX*, *FN1*, *POSTN*, *TNC*, *ACTA2*, *THBS1*, *ITGA5*, *ITGB1*, *PXN*, and *VCL* [15–18]. This signature consists of genes associated with ECM structure, crosslinking, fibroblasts and cell adhesion. It was therefore regarded as a transcriptomic surrogate for ECM/stromal remodeling rather than a direct measurement of tissue stiffness or elastic modulus.

Single-sample gene set enrichment analysis (ssGSEA) [19] was applied to calculate the ECM/stromal remodeling score for each tumor. Scores were compared across the median-defined FOXA2 expression groups, and associations with continuous FOXA2 expression were evaluated using Spearman correlation. Survival associations were examined using continuous-score models and median-stratified groups for visualization. To address tumor-purity confounding, purity-adjusted partial Spearman correlations were specified for FOXA2 versus the ECM/stromal remodeling score and for representative ECM/stromal genes, using only tumors with matched FOXA2 expression, signature or gene expression, and tumor-purity data.

2.7 FAK–YAP-Related Transcriptional Signature Analysis

A FAK–YAP-related transcriptional signature comprising *PTK2*, *YAP1*, *WWTR1*, *TEAD1*, *TEAD4*, *CTGF*, *CYR61*, *ANKRD1*, *AMOTL2*, *ITGB1*, *PXN*, and *VCL* was quantified using ssGSEA [20, 21]. This score was regarded as a mechanotransduction-related transcriptional signature. It cannot directly reflect FAK phosphorylation, YAP/TAZ nuclear localization, TEAD binding or pathway activation.

Correlations between FOXA2 expression and *PTK2*, *YAP1*, *WWTR1*, *CTGF*, *CYR61* and *ANKRD1* were assessed using Spearman correlation. The association between the ECM/stromal remodeling score and the FAK–YAP-related score was also evaluated. Because *ITGB1*, *PXN* and *VCL* are present in both signatures, a sensitivity analysis was defined in which these three overlapping genes were removed from both gene sets, the two single-sample scores were recalculated, and their association was reassessed using Spearman correlation. This overlap-excluded analysis was intended to distinguish correlation attributable to shared gene content from correlation between the remaining transcriptional features.

2.8 Tumor Microenvironment Estimation

The ESTIMATE algorithm [22] was applied to calculate stromal, immune and overall ESTIMATE scores and to derive tumor purity using the published transformation formula:

$$\text{TumorPurity} = \cos\left(a + b \times S\right), \tag{1}$$

where S is the ESTIMATE score of a sample, $a = 0.6049872018$ and $b = 0.0001467884$. The resulting tumor-microenvironment table was organized at the individual-sample level, with TCGA sample identifiers matched to the expression matrix and with StromalScore, ImmuneScore, ESTIMATEScore and TumorPurity retained as separate variables. TumorPurity was analyzed on its 0–1 scale and was not treated as a percentage or as interchangeable with the raw ESTIMATE score. Immune cell fractions were calculated via CIBERSORT [23] only when all input requirements were satisfied. Outputs from the CIBERSORT LM22 leukocyte signature matrix were limited to its compatible leukocyte subsets. For descriptive trend visualization, tumors were additionally grouped into FOXA2 expression quartiles (Q1–Q4).

Fibroblast and endothelial signatures were assessed via single-sample gene set scoring and were not regarded as cell fractions derived from CIBERSORT. Representative molecular markers included *ACTA2*, *FAP*, *PDGFRB*, *COL1A1*, *COL3A1*, *CD68*, *CD163*, *MRC1*, *CD8A*, *PDCD1*, *CD274*, *CTLA4*, *HAVCR2*, *TIGIT*, and *LAG3*. Scores generated by different algorithms were analyzed separately, and these values were not considered to represent an absolute 100% cellular composition.

2.9 Statistical Analysis

Continuous variables were presented as mean ± standard deviation or median with interquartile range in accordance with their distribution patterns. Paired and unpaired comparisons were performed using the paired Wilcoxon signed-rank test and Wilcoxon rank-sum test, respectively, unless parametric assumptions were met. Categorical variables were compared using the chi-square test or Fisher's exact test, as appropriate.

Kaplan–Meier curves were compared with the log-rank test. Cox proportional hazards regression

Table 1. Public datasets included in this study and their analytical purposes.

Dataset	Source	Platform	Sample profile	Main analytical use
TCGA-LIHC	The Cancer Genome Atlas	RNA-seq	374 HCC tissues and 50 adjacent non-tumor tissues	Discovery cohort for expression, survival, differential expression, pathway scoring, and tumor microenvironment analyses
ICGC-LIRI-JP	International Cancer Genome Consortium	RNA-seq	240 HCC tissues and 202 non-tumor liver tissues	External validation of FOXA2 expression and supportive molecular associations
GSE14520	Gene Expression Omnibus	Affymetrix microarray	488 total liver samples, including HCC and paired non-tumor tissues	External validation of FOXA2 expression where platform and sample annotations were compatible

Note: Dataset counts correspond to the source files used in the analysis. Cohorts were analyzed separately, and expression values from RNA-sequencing and microarray platforms were not pooled.

was used for prognostic analysis, and the proportional hazards assumption was assessed using Schoenfeld residuals. Spearman correlation coefficients (ρ) were used for unadjusted correlation analyses. For the tumor-purity sensitivity analysis, partial Spearman correlation was used to assess FOXA2–ECM/stromal and FOXA2–FAK–YAP associations while controlling for the matched tumor-purity value. The effective sample size for each adjusted analysis was defined after matching TCGA sample identifiers across the expression matrix, signature scores and tumor-purity table; samples missing any required variable were excluded only from that specific analysis. Benjamini–Hochberg correction was applied to prespecified sets of multiple tests. All statistical tests were two-sided.

3 Results

3.1 Public HCC Datasets and Analysis Populations

The public datasets adopted for transcriptomic analyses are summarized in Table 1. The TCGA-LIHC cohort served as the discovery cohort and contained 374 primary HCC tumor samples and 50 adjacent non-tumor samples in the expression dataset. Tumor-only molecular analyses started from the 374 primary tumors, with the effective sample size determined by availability of the variables required for each analysis. Among these tumors, 364 cases had the information required for the median-group survival and clinicopathological analyses presented in the current figures and tables. The ICGC-LIRI-JP and GSE14520 datasets provided external evidence for the direction of FOXA2 expression changes.

Cross-cohort analyses were performed separately to prevent direct pooling of expression values from RNA-sequencing and microarray platforms. External datasets were mainly applied to validate the reproducibility of FOXA2 downregulation. All core prognostic and tumor microenvironmental analyses were based on the TCGA-LIHC cohort unless otherwise specified.

3.2 FOXA2 Is Downregulated in HCC and Associated With Adverse Clinical Features

FOXA2 expression was lower in HCC tissues than in adjacent non-tumor liver tissues in the paired analysis of the TCGA-LIHC cohort (Figure 1(A)). The same expression pattern was also found in the full unpaired TCGA-LIHC cohort, ICGC-LIRI-JP and GSE14520 (Figure 1(B)). Since expression scales and sample composition varied across different platforms, these results were regarded as directional replication rather than a pooled effect estimate.

In Kaplan–Meier analyses using the cohort-specific median FOXA2 expression value as the cutoff, patients in the FOXA2-high group exhibited better overall survival than those in the FOXA2-low group (log-rank $P = 0.006$; hazard ratio [HR] for high versus low expression $= 0.57$, 95% confidence interval [CI] 0.39–0.85, equivalent to HR $= 1.74$ for low versus high expression in Table 3; Figure 1(C)). FOXA2 expression was also lower in samples with advanced tumor stage, high histological grade or vascular invasion (Figure 1(D)). These associations do not establish that reduced FOXA2 directly drives disease progression and may also reflect differences in tumor differentiation, tumor purity or stromal composition.

Table 2 presents descriptive associations in the 364 TCGA-LIHC cases used for the median-group comparison. The FOXA2-low group had larger proportions of cases with advanced tumor stage, high histological grade, positive vascular invasion, elevated

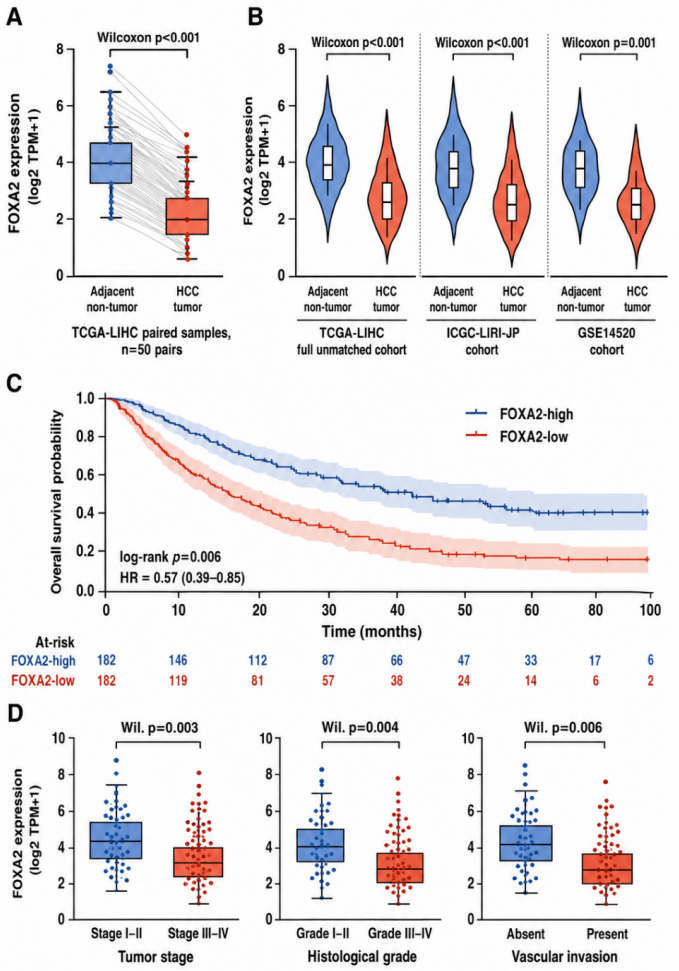

Figure 1. Expression and clinical associations of FOXA2 in hepatocellular carcinoma. (A) Paired comparison of FOXA2 expression between HCC and adjacent non-tumor tissues in TCGA-LIHC. (B) Separate expression comparisons in TCGA-LIHC, ICGC-LIRI-JP, and GSE14520; values were not pooled across platforms. (C) Kaplan–Meier overall survival analysis using the cohort-specific median FOXA2 expression value as the cutoff for FOXA2-low and FOXA2-high groups. (D) Associations between FOXA2 expression and available clinicopathological variables. Sample sizes vary according to annotation availability.

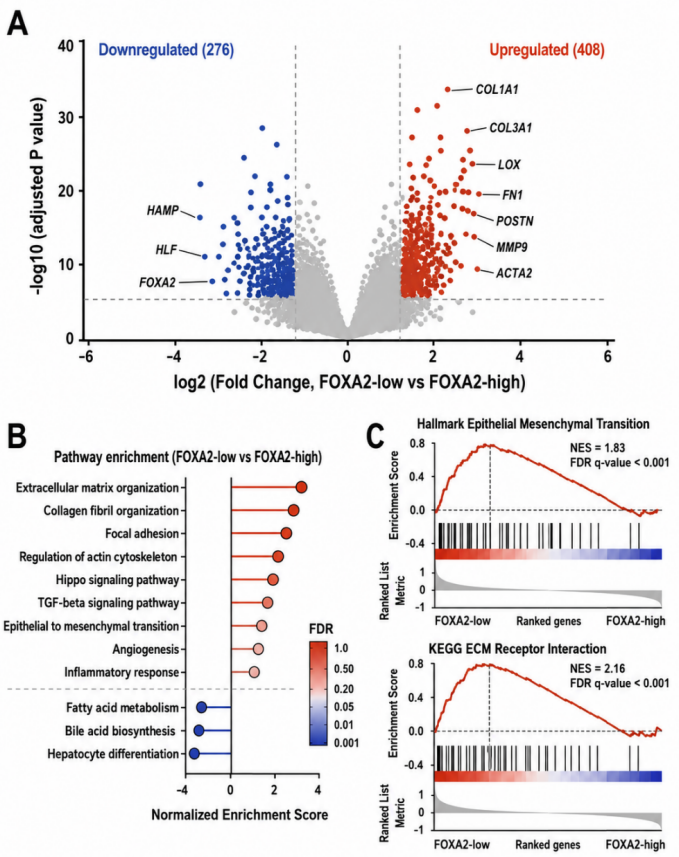

Figure 2. FOXA2-associated transcriptional states in hepatocellular carcinoma. (A) Differential expression between median-defined FOXA2-low and FOXA2-high tumors. (B) Selected functional enrichment results. (C) GSEA of epithelial–mesenchymal transition and ECM–receptor interaction. Enrichment indicates association with the FOXA2 expression state and does not establish direct FOXA2 target regulation.

AFP levels and mortality events. High ECM/stromal remodeling and FAK–YAP-related transcriptional scores were also more frequent in the FOXA2-low group. These comparisons arise from the same bulk expression matrix and were not interpreted as independent mechanistic evidence.

3.3 FOXA2-Low Tumors Are Associated With ECM Remodeling and Loss-of-Differentiation Transcriptional Features

Differential expression analysis stratified by median FOXA2 expression identified 408 upregulated and 276 downregulated genes in FOXA2-low tumors according to the predefined reporting thresholds (Figure 2(A)). ECM- and stromal-associated genes, including *COL1A1*, *COL3A1*, *LOX*, *FN1*, *POSTN*, *MMP9*, and *ACTA2*, were expressed at higher levels in the FOXA2-low group. The expression of FOXA2 and hepatocyte-associated genes was decreased. In bulk tissue samples, this expression pattern may reflect alterations in both tumor-cell status and stromal abundance.

Pathway enrichment analysis showed positive enrichment of transcriptional programs related to extracellular matrix organization, collagen fibril organization, focal adhesion, regulation of the actin cytoskeleton, Hippo signaling, transforming growth factor-β (TGF-β) signaling, EMT, angiogenesis, and inflammatory response in FOXA2-low tumors (Figure 2(B)). Fatty acid metabolism, bile acid biosynthesis, and hepatocyte differentiation showed negative enrichment. The coexistence of stromal

Table 2. Descriptive associations between FOXA2 expression groups and clinicopathological or transcriptomic features in TCGA-LIHC.

Variable	Category	FOXA2-low ($n = 182$)	FOXA2-high ($n = 182$)	P value
Age	< 60 years	78 (42.9%)	82 (45.1%)	0.672
	≥ 60 years	104 (57.1%)	100 (54.9%)	
Sex	Male	125 (68.7%)	119 (65.4%)	0.503
	Female	57 (31.3%)	63 (34.6%)	
Tumor stage	I–II	111 (61.0%)	138 (75.8%)	0.003
	III–IV	71 (39.0%)	44 (24.2%)	
Histological grade	Grade I–II	91 (50.0%)	118 (64.8%)	0.004
	Grade III–IV	91 (50.0%)	64 (35.2%)	
Vascular invasion	Absent	96 (52.7%)	122 (67.0%)	0.006
	Present	86 (47.3%)	60 (33.0%)	
Serum AFP	< 400 ng/mL	103 (56.6%)	126 (69.2%)	0.013
	≥ 400 ng/mL	79 (43.4%)	56 (30.8%)	
Survival status	Alive	104 (57.1%)	130 (71.4%)	0.004
	Dead	78 (42.9%)	52 (28.6%)	
ECM/stromal remodeling score	Low	63 (34.6%)	119 (65.4%)	< 0.001
	High	119 (65.4%)	63 (34.6%)	
FAK–YAP score	Low	70 (38.5%)	112 (61.5%)	< 0.001
	High	112 (61.5%)	70 (38.5%)	

Note: Analyses are descriptive and use the cohort-specific median FOXA2 expression value to define two groups of equal size ($n = 182$ per group; total $n = 364$). AFP, alpha-fetoprotein.

enrichment and suppressed hepatocyte-related programs is compatible with a poorly differentiated and/or lower-purity bulk tumor phenotype.

GSEA revealed enrichment of the hallmark EMT and KEGG ECM–receptor interaction gene sets in FOXA2-low tumors (Figure 2(C)). Exploratory enrichment additionally indicated negative enrichment of lipid metabolism-related programs, including fatty acid metabolism and bile acid biosynthesis, in FOXA2-low tumors (Figure 2(B)); these findings are consistent with loss of hepatocyte metabolic identity but require independent validation. These findings characterize a FOXA2-associated transcriptional state but do not establish direct FOXA2 binding or transcriptional repression of the enriched pathways.

3.4 Low FOXA2 Expression Is Associated With an ECM/Stromal Remodeling Signature

The predefined ECM/stromal remodeling signature was expressed at higher levels in FOXA2-low tumors (Figure 3(A)). This signature consists of genes related to ECM structure, crosslinking, fibroblasts and cell adhesion; accordingly, it was regarded as a bulk transcriptomic remodeling score rather than a direct measure of matrix stiffness.

FOXA2 expression showed inverse unadjusted Spearman correlations with representative ECM/stromal genes, including *COL1A1*, *LOX*, *FN1*, *POSTN*, and *ACTA2* (Figure 3(B)). Because FOXA2 expression and these stromal genes are both sensitive to the relative abundance of hepatocyte-lineage and non-tumor cells, these plotted coefficients represent unadjusted bulk-tissue associations. The purity-adjusted analysis should therefore be interpreted from the matched-sample partial Spearman estimates rather than from the unadjusted coefficients alone.

The ECM/stromal remodeling score was higher in FOXA2-low tumors than in FOXA2-high tumors, and the group with a high median-stratified score had poorer overall survival (Figure 3(C)). These findings support an association between the ECM/stromal transcriptional state and prognosis but do not indicate that FOXA2 directly regulates tissue stiffness.

3.5 FOXA2 Expression Is Inversely Associated With a FAK–YAP-Related Transcriptional Signature

FOXA2 expression showed an inverse correlation with the expression of *PTK2*, *YAP1*, *WWTR1*, *CTGF*, *CYR61* and *ANKRD1* in the TCGA-LIHC cohort (Figure 4(A)). These associations at the mRNA level are consistent with a mechanotransduction-related transcriptional state, yet they cannot confirm FAK phosphorylation,

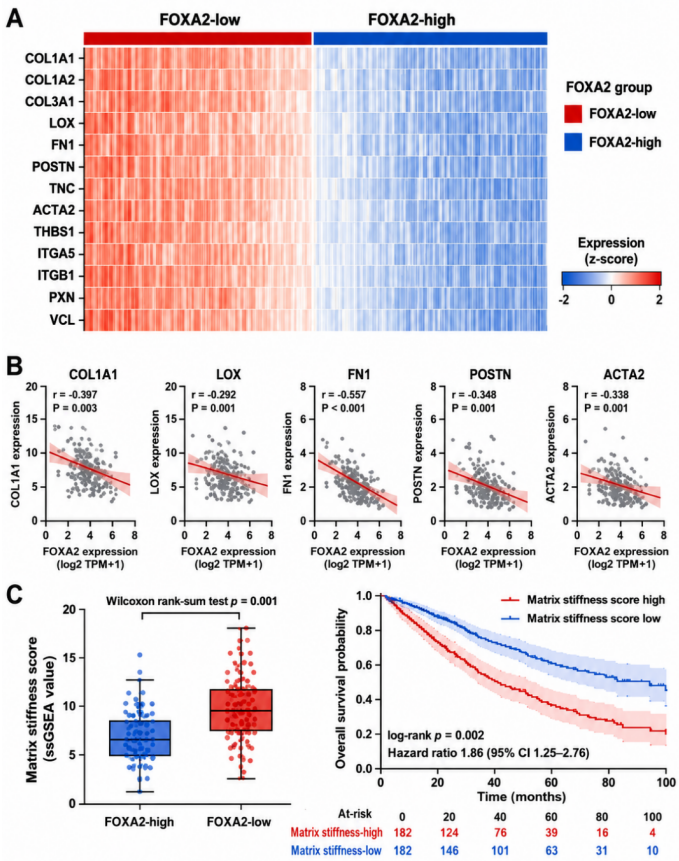

Figure 3. Association of FOXA2 with an ECM/stromal remodeling-related transcriptional signature. (A) Expression heatmap of signature genes. (B) Unadjusted Spearman correlations between FOXA2 and representative ECM/stromal genes. (C) Score comparison and median-group overall survival analysis. The score is a transcriptomic surrogate and not a direct measurement of matrix elastic modulus.

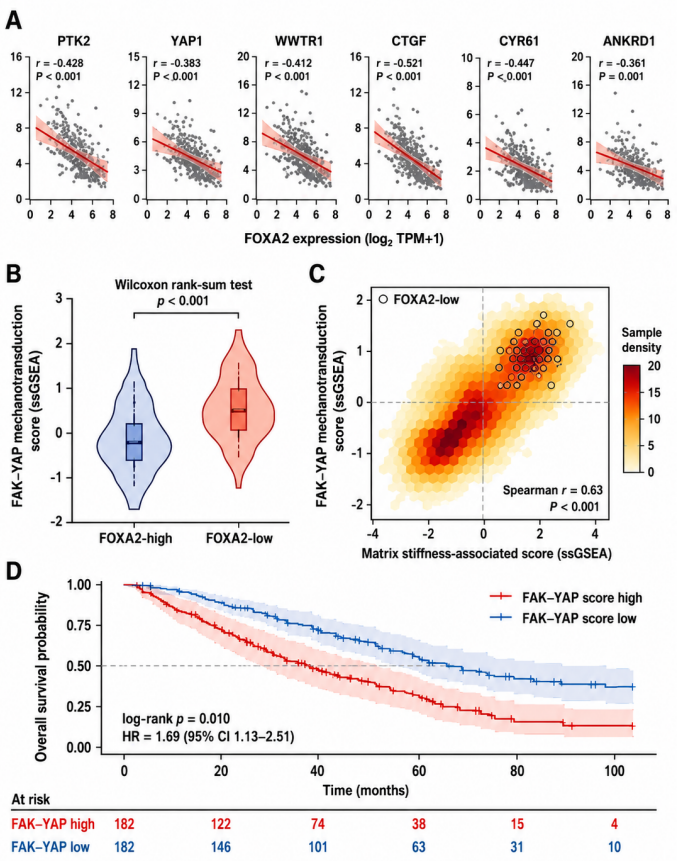

Figure 4. Relationship between FOXA2 expression and a FAK–YAP-related transcriptional signature. (A) Spearman correlations with selected genes. (B) Score comparison between median-defined FOXA2 groups. (C) Unadjusted association between the original ECM/stromal remodeling and FAK–YAP-related scores; the two signatures share *ITGB1*, *PXN* and *VCL*. (D) Median-group overall survival analysis. Transcript abundance does not directly measure FAK phosphorylation or YAP/TAZ protein activity.

YAP/TAZ nuclear localization or direct pathway activation.

The FAK–YAP-related transcriptional score was higher in FOXA2-low tumors (Figure 4(B)). The original ECM/stromal remodeling score and FAK–YAP-related score were positively correlated (Spearman $\rho = 0.63$, $P < 0.001$; Figure 4(C)). Because *ITGB1*, *PXN* and *VCL* are included in both original signatures, this unadjusted coefficient can be inflated by shared gene content. The overlap-excluded sensitivity analysis therefore requires recalculation of both scores after removing *ITGB1*, *PXN* and *VCL* before the magnitude of the ECM–FAK–YAP association is interpreted biologically.

Patients with high FAK–YAP-related scores had worse overall survival in the median-based comparison (Figure 4(D)). In the multivariable model presented in Table 3, low FOXA2 expression, high ECM/stromal remodeling score, and advanced tumor stage were associated with adverse overall survival, whereas the association for a high FAK–YAP-related score was borderline (lower confidence limit 1.00). Because the transcriptomic predictors are correlated bulk-expression features and several estimates are close to the null boundary, this multivariable model was interpreted as exploratory.

3.6 FOXA2 Expression Is Associated With Inferred Immune-Stromal Features

FOXA2-low tumors had higher scores for fibroblast, M2 macrophage, regulatory T-cell and endothelial signatures, along with lower scores for CD8-positive T-cell and M1 macrophage signatures (Figure 5(A)). These estimates were derived from transcriptomic data and do not equal cell counts measured via histology. Fibroblast and endothelial signatures were analyzed

Table 3. Exploratory Cox regression analysis of overall survival in TCGA-LIHC.

Variable	Category	Univariable HR (95% CI)	P value	Multivariable HR (95% CI)	P value
FOXA2 expression	Low vs high	1.74 (1.17–2.58)	0.006	1.48 (1.02–2.24)	0.051
ECM/stromal remodeling score	High vs low	1.86 (1.25–2.76)	0.002	1.59 (1.06–2.39)	0.027
FAK–YAP score	High vs low	1.69 (1.13–2.51)	0.010	1.45 (1.00–2.19)	0.063
Age	≥ 60 vs < 60 years	1.12 (0.78–1.61)	0.536	1.08 (0.74–1.57)	0.695
Sex	Male vs female	1.09 (0.72–1.66)	0.682	1.05 (0.68–1.63)	0.824
Tumor stage	III–IV vs I–II	2.23 (1.49–3.33)	< 0.001	1.91 (1.24–2.94)	0.004
Histological grade	III–IV vs I–II	1.39 (0.97–2.00)	0.068	1.21 (0.83–1.78)	0.323
Vascular invasion	Present vs absent	1.64 (1.07–2.52)	0.025	1.37 (0.87–2.16)	0.174
Serum AFP	≥ 400 vs < 400 ng/mL	1.42 (0.97–2.09)	0.071	1.26 (0.84–1.90)	0.263

Note: HR, hazard ratio; CI, confidence interval; AFP, alpha-fetoprotein. The multivariable model is exploratory because the FOXA2 and transcriptomic signature variables are correlated and several confidence intervals approach 1.0. P values for FOXA2 expression and FAK–YAP score in the multivariable model are approximated from the reported HR and 95% CI and should be verified against the primary analysis output.

independently of leukocyte fractions calculated by CIBERSORT.

FOXA2 expression showed inverse correlations with multiple stromal and immune-checkpoint-related signatures, while ECM/stromal remodeling and FAK–YAP-related scores were positively correlated with these features (Figure 5(B)). Shared genes, tumor purity and cellular composition may contribute to these associations. The heatmap was therefore interpreted as descriptive evidence of a coordinated expression state in bulk tissues and not as evidence of directionality or causation.

ESTIMATE-derived stromal, immune and composite scores differed across FOXA2 expression quartiles (Figure 5(C)), consistent with greater abundance of stromal and immune transcripts in FOXA2-low tumors. The raw ESTIMATE score scale is distinct from the 0–1 tumor-purity transformation (Equation (1)). The composite plot in Figure 5(D) is descriptive: values generated by different algorithms do not represent absolute cellular fractions and cannot be interpreted as a validated 100% cellular composition.

Taken together, the ECM/stromal remodeling, FAK–YAP-related transcriptional, and immune-stromal findings represent correlated transcriptional characteristics measured in the same bulk HCC specimens. The analyses do not demonstrate that ECM remodeling precedes or causes FAK–YAP activation, nor that either feature causes the observed immune pattern; these relationships require cell-type-resolved and functional validation.

4 Discussion

This study identified consistent downregulation of FOXA2 in HCC together with associations between low FOXA2 expression, unfavorable clinical outcomes, ECM/stromal remodeling, FAK–YAP-related transcription and inferred immune-stromal features [24, 25]. These findings describe a coordinated expression pattern in bulk tissues but do not verify a causal FOXA2–matrix stiffness–FAK–YAP axis.

FOXA2 plays a core role in maintaining hepatocyte lineage identity, chromatin accessibility and metabolic regulation. Its decreased expression in HCC may therefore indicate loss of hepatocyte differentiation. In the current analysis, low FOXA2 expression was associated with advanced clinicopathological characteristics and poorer survival. However, FOXA2 levels in bulk tissues can also be influenced by tumor purity and the relative proportions of hepatocyte-lineage, stromal and immune cells. Accordingly, the observed prognostic and microenvironmental associations may contain a cellular-composition component and should not be interpreted as purely tumor-intrinsic.

FOXA2-low tumors exhibited enrichment of transcriptional programs related to ECM, collagen, fibroblasts, focal adhesion, TGF-β signaling, Hippo signaling and EMT, alongside suppression of metabolic and hepatocyte-differentiation programs. This pattern is compatible with HCC samples characterized by abundant stroma and reduced hepatocyte differentiation. It does not establish that FOXA2 directly represses ECM-related genes. Single-cell analyses, spatial profiling and direct transcription-factor binding assays are required to distinguish tumor-cell regulation from changes in cellular composition [26–28].

The inverse association between FOXA2 expression and the FAK–YAP-related score provides a hypothesis for subsequent mechanistic research.

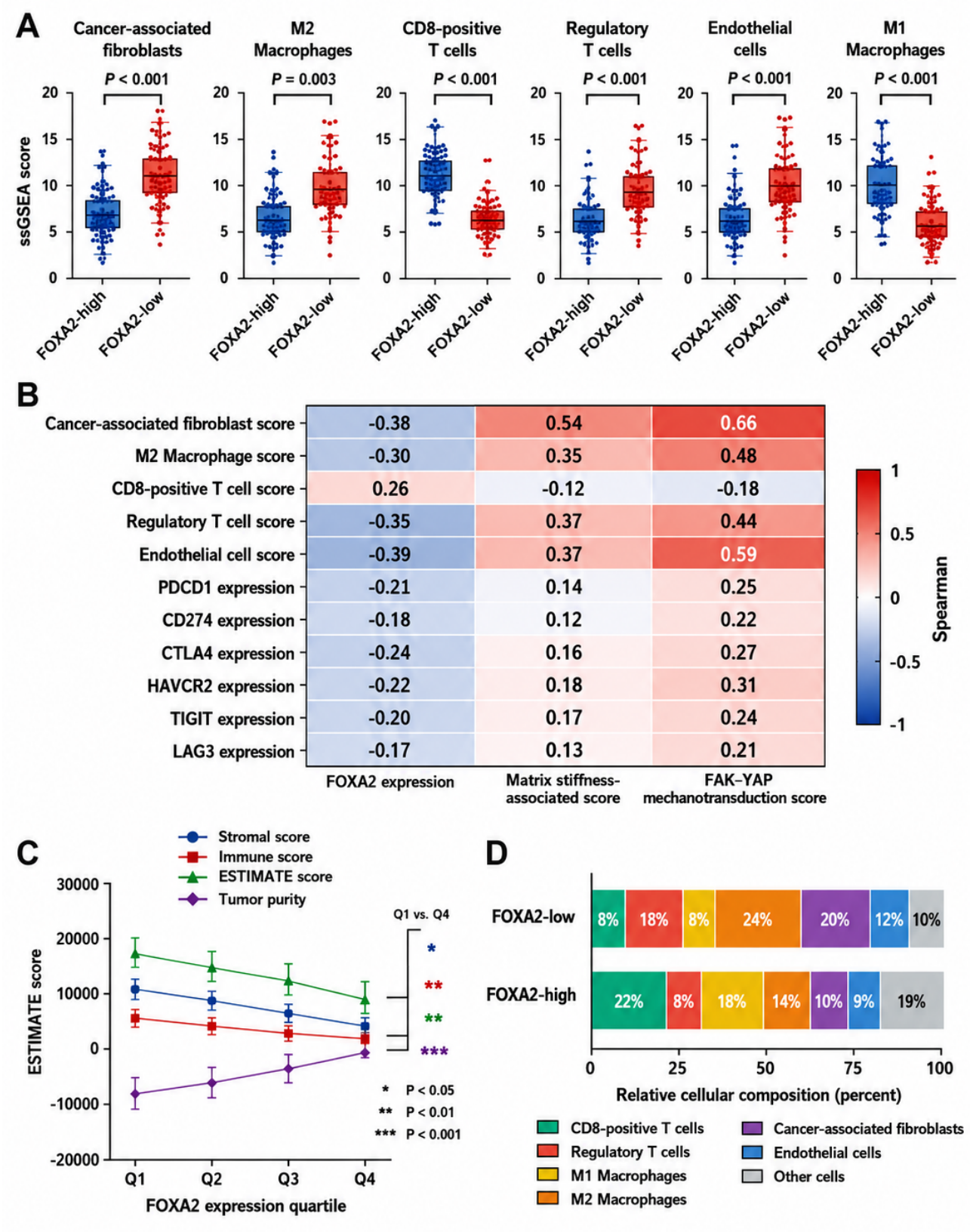

Figure 5. Inferred tumor microenvironment features associated with FOXA2 expression. (A) Comparison of transcriptome-derived immune and stromal signature scores. (B) Spearman correlation heatmap. (C) ESTIMATE-derived score trends across FOXA2 expression quartiles; the raw ESTIMATE scale is distinct from the 0–1 tumor-purity transformation. (D) Descriptive composite visualization; values generated from different signature methods do not represent absolute deconvolved cellular proportions.

Prior experimental studies show that increased matrix stiffness can activate integrin–FAK signaling and promote YAP nuclear translocation [29, 30], but those protein-level events are not measured by the mRNA data analyzed here. In addition, the ECM/stromal and FAK–YAP-related signatures share *ITGB1*, *PXN* and *VCL*, which can inflate their unadjusted score correlation. Thus, the observed transcriptional association does not demonstrate that ECM remodeling activates FAK–YAP signaling in these samples. Protein-level detection of phosphorylated FAK (p-FAK), nuclear YAP/TAZ and TEAD targets, together with stiffness-controlled functional experiments, would be needed to test that mechanism.

FOXA2-low tumors also presented transcriptomic features linked to fibroblasts, M2 macrophages, regulatory T cells, endothelial cells and immune checkpoint molecules. This pattern is compatible with immunosuppressive or immune-excluded transcriptional characteristics, consistent with prior reports that macrophage–fibroblast crosstalk shapes tumor barriers, immune exclusion zones, and onco-fetal neighborhoods that collectively impair anti-tumor immunity and modulate immunotherapy response in HCC [31–33]. However, the deconvolution results depend on selected reference signatures and do not demonstrate functional immune suppression or predict response to immune checkpoint blockade [23]. Validation using independent deconvolution methods, histological approaches or single-cell sequencing is therefore warranted.

Several limitations should guide interpretation. First, this retrospective study is based on bulk transcriptomic data and therefore does not establish causality, cellular origin, matrix stiffness, FAK phosphorylation or YAP localization. Second, tumor purity, hepatocyte differentiation and stromal abundance can confound correlations between FOXA2 and microenvironmental signatures. Third, the two core signatures share three genes, which can inflate their correlation, and the prognostic models involve correlated transcriptomic predictors. Fourth, immune and stromal cell estimates were generated using different transcriptomic approaches and are not absolute cellular percentages. Fifth, FOXA2 has context-dependent functions in HCC, including reported roles in tumor progression and treatment resistance [10]. Finally, the absence of protein-level, single-cell, spatial and functional validation limits mechanistic interpretation.

Collectively, these results support FOXA2 expression as a candidate biomarker of differentiation status and microenvironment-associated transcriptional features in HCC. ECM/stromal remodeling, FAK–YAP-related transcription and immune-stromal features were observed as correlated characteristics within the same bulk tumors; the present analysis does not establish a temporal or causal sequence among them. Direct regulatory interactions therefore remain to be tested experimentally.

5 Conclusion

Low FOXA2 expression was associated with unfavorable clinical outcomes, ECM/stromal remodeling, FAK–YAP-related transcriptional features, and an immune-stromal-enriched bulk expression profile in HCC. These findings support FOXA2 as a candidate marker for biological stratification but do not demonstrate that FOXA2 regulates matrix stiffness, activates FAK–YAP signaling, or drives immune remodeling. Further validation in cell-type-resolved, protein-level and functional models is needed to determine the underlying mechanism and clinical relevance.

Data Availability Statement

All datasets analyzed in this study are publicly available from TCGA/GDC (TCGA-LIHC), the International Cancer Genome Consortium (ICGC-LIRI-JP), and the Gene Expression Omnibus (GSE14520). No new primary sequencing dataset was generated in this study. Gene-signature definitions are provided in the Methods section. Analysis code and processed intermediate files are not publicly deposited but are available from the corresponding author upon reasonable request.

Funding

This work was supported without any funding.

Conflicts of Interest

The authors declare no conflicts of interest.

AI Use Statement

The authors declare that no generative AI was used in the preparation of this manuscript.

Ethical Approval and Consent to Participate

This study analyzed only publicly available, de-identified data from the TCGA, ICGC and GEO

repositories. Ethical approval and informed consent were obtained by the investigators who conducted the original studies that generated these data, and no additional human participants were recruited for the present study. The secondary use of these public data was reviewed by the Ethics Committee of Sichuan University (approval No. 202503T013), and the study was conducted in accordance with the Declaration of Helsinki.

References

[1] Feng, F., & Zhao, Y. (2024). Hepatocellular carcinoma: Prevention, diagnosis, and treatment. *Medical Principles and Practice, 33*(5), 414-423. [CrossRef]

[2] Roy, A. M., Iyer, R., & Chakraborty, S. (2023). The extracellular matrix in hepatocellular carcinoma: Mechanisms and therapeutic vulnerability. *Cell Reports Medicine, 4*(9), 101170. [CrossRef]

[3] Hong, J., Yu, J., Buratto, D., Chen, W., Zhou, R., Ling, S., & Xu, X. (2024). Unveiling the role of mechanical microenvironment in hepatocellular carcinoma: molecular mechanisms and implications for therapeutic strategies. *International Journal of Biological Sciences, 20*(13), 5239. [CrossRef]

[4] Zhang, M., & Zhang, B. (2025). Extracellular matrix stiffness: mechanisms in tumor progression and therapeutic potential in cancer. *Experimental hematology & oncology, 14*(1), 54. [CrossRef]

[5] Mai, Z., Lin, Y., Lin, P., Zhao, X., & Cui, L. (2024). Modulating extracellular matrix stiffness: A strategic approach to boost cancer immunotherapy. *Cell Death & Disease, 15*(5), 307. [CrossRef]

[6] Li, S., Hao, L., Li, N., Hu, X., Yan, H., Dai, E., & Shi, X. (2024). Targeting the Hippo/YAP1 signaling pathway in hepatocellular carcinoma: From mechanisms to therapeutic drugs (Review). *International Journal of Oncology, 65*(3), 88. [CrossRef]

[7] Gao, Y., Gong, Y., Lu, J., Hao, H., & Shi, X. (2024). Targeting YAP1 to improve the efficacy of immune checkpoint inhibitors in liver cancer: mechanism and strategy. *Frontiers in Immunology, 15*, 1377722. [CrossRef]

[8] Xia, Y., Liang, P., Cui, L., & Cao, Y. (2026). FOXA2 in cancer: from fundamental biology to clinical translation. *Frontiers in Oncology, 16*, 1854448. [CrossRef]

[9] Liu, N., Wang, A., Xue, M., Zhu, X., Liu, Y., & Chen, M. (2024). FOXA1 and FOXA2: the regulatory mechanisms and therapeutic implications in cancer. *Cell death discovery, 10*(1), 172. [CrossRef]

[10] Wang, Z., Shen, J., Chen, C., Wen, T., & Li, C. (2023). FOXA2 plays a critical role in hepatocellular carcinoma progression and lenvatinib-associated drug resistance. *BioScience Trends, 17*(2), 136-147. [CrossRef]

[11] Ally, A., Balasundaram, M., Carlsen, R., Chuah, E., Clarke, A., Dhalla, N., ... & Ferguson, M. L. (2017). Comprehensive and integrative genomic characterization of hepatocellular carcinoma. *Cell, 169*(7), 1327-1341. [CrossRef]

[12] Fujimoto, A., Furuta, M., Totoki, Y., Tsunoda, T., Kato, M., Shiraishi, Y., ... & Nakagawa, H. (2016). Whole-genome mutational landscape and characterization of noncoding and structural mutations in liver cancer. *Nature genetics, 48*(5), 500-509. [CrossRef]

[13] Roessler, S., Jia, H. L., Budhu, A., Forgues, M., Ye, Q. H., Lee, J. S., ... & Wang, X. W. (2010). A unique metastasis gene signature enables prediction of tumor relapse in early-stage hepatocellular carcinoma patients. *Cancer Research, 70*(24), 10202-10212. [CrossRef]

[14] Subramanian, A., Tamayo, P., Mootha, V. K., Mukherjee, S., Ebert, B. L., Gillette, M. A., ... & Mesirov, J. P. (2005). Gene set enrichment analysis: a knowledge-based approach for interpreting genome-wide expression profiles. *Proceedings of the National Academy of Sciences, 102*(43), 15545-15550. [CrossRef]

[15] Li, H., Zhang, J., Shi, Y., Wang, H., Yang, R., Wu, S., ... & Sun, L. (2025). Identification of matrix stiffness-related molecular subtypes in HCC via integrating multi-omics analysis and machine learning algorithms. *Journal of Translational Medicine, 23*(1), 716. [CrossRef]

[16] Shen, Y., Chen, J., Zhou, Z., Wu, J., Hu, X., Xu, Y., ... & Xu, X. (2024). Matrix stiffness-related extracellular matrix signatures and the DYNLL1 protein promote hepatocellular carcinoma progression through the Wnt/β-catenin pathway. *BMC Cancer, 24*(1), 1211. [CrossRef]

[17] Liu, H. H., Xu, Y., Gao, W. Q., Li, J. J., Zhang, R., Chen, M. P., ... & Chen, R. X. (2025). Matrix Stiffness Promotes Invasion and Metastasis of Hepatocellular Carcinoma via a New Mechanoresponsive SCD1/HMMR Pathway. *The FASEB Journal, 39*(11), e70716. [CrossRef]

[18] Wang, Z., Wang, W., Luo, Q., & Song, G. (2025). High matrix stiffness accelerates migration of hepatocellular carcinoma cells through the integrin β1-Plectin-F-actin axis. *BMC Biology, 23*(1), 8. [CrossRef]

[19] Barbie, D. A., Tamayo, P., Boehm, J. S., Kim, S. Y., Moody, S. E., Dunn, I. F., ... & Hahn, W. C. (2009). Systematic RNA interference reveals that oncogenic KRAS-driven cancers require TBK1. *Nature, 462*(7269), 108-112. [CrossRef]

[20] Yan, W., Xiao, G. H., Wang, L. J., Zhou, Y., Yang, F., & Mou, K. H. (2025). CAFs activated by YAP1 upregulate cancer matrix stiffness to mediate hepatocellular carcinoma progression. *Journal of translational medicine, 23*(1), 450. [CrossRef]

[21] Kim, H. S., & Nam, J. S. (2025). The multifaceted

role of YAP in the tumor microenvironment and its therapeutic implications in cancer. *Experimental & Molecular Medicine, 57*(10), 2201-2213. [CrossRef]

[22] Yoshihara, K., Shahmoradgoli, M., Martínez, E., Vegesna, R., Kim, H., Torres-Garcia, W., ... & Verhaak, R. G. (2013). Inferring tumour purity and stromal and immune cell admixture from expression data. *Nature communications, 4*(1), 2612. [CrossRef]

[23] Newman, A. M., Liu, C. L., Green, M. R., Gentles, A. J., Feng, W., Xu, Y., ... & Alizadeh, A. A. (2015). Robust enumeration of cell subsets from tissue expression profiles. *Nature methods, 12*(5), 453-457. [CrossRef]

[24] Shen, K. Y., Zhu, Y., Xie, S. Z., & Qin, L. X. (2024). Immunosuppressive tumor microenvironment and immunotherapy of hepatocellular carcinoma: current status and prospectives. *Journal of hematology & oncology, 17*(1), 25. [CrossRef]

[25] Fu, Y., Guo, X., Sun, L., Cui, T., Wu, C., Wang, J., ... & Liu, L. (2024). Exploring the role of the immune microenvironment in hepatocellular carcinoma: Implications for immunotherapy and drug resistance. *Elife, 13*, e95009. [CrossRef]

[26] Ma, L., Hernandez, M. O., Zhao, Y., Mehta, M., Tran, B., Kelly, M., ... & Wang, X. W. (2019). Tumor cell biodiversity drives microenvironmental reprogramming in liver cancer. *Cancer cell, 36*(4), 418-430. [CrossRef]

[27] Wu, R., Guo, W., Qiu, X., Wang, S., Sui, C., Lian, Q., ... & Chen, L. (2021). Comprehensive analysis of spatial architecture in primary liver cancer. *Science advances, 7*(51), eabg3750. [CrossRef]

[28] Wederell, E. D., Bilenky, M., Cullum, R., Thiessen, N., Dagpinar, M., Delaney, A., ... & Hoodless, P. A. (2008). Global analysis of in vivo Foxa2-binding sites in mouse adult liver using massively parallel sequencing. *Nucleic acids research, 36*(14), 4549-4564. [CrossRef]

[29] Sleeboom, J. J. F., van Tienderen, G. S., Schenke-Layland, K., van der Laan, L. J. W., Khalil, A. A., & Verstegen, M. M. A. (2024). The extracellular matrix as hallmark of cancer and metastasis: From biomechanics to therapeutic targets. *Science Translational Medicine, 16*(728), eadg3840. [CrossRef]

[30] Dupont, S., Morsut, L., Aragona, M., Enzo, E., Giulitti, S., Cordenonsi, M., ... & Piccolo, S. (2011). Role of YAP/TAZ in mechanotransduction. *Nature, 474*(7350), 179-183. [CrossRef]

[31] Long, F., Zhong, W., Zhao, F., Xu, Y., Hu, X., Jia, G., ... & Wang, F. (2024). DAB2+ macrophages support FAP+ fibroblasts in shaping tumor barrier and inducing poor clinical outcomes in liver cancer. *Theranostics, 14*(12), 4822. [CrossRef]

[32] Liu, Y., Xun, Z., Ma, K., Liang, S., Li, X., Zhou, S., ... & Liu, L. (2023). Identification of a tumour immune barrier in the HCC microenvironment that determines the efficacy of immunotherapy. *Journal of hepatology, 78*(4), 770-782. [CrossRef]

[33] Li, Z., Pai, R., Gupta, S., Currenti, J., Guo, W., Di Bartolomeo, A., ... & Sharma, A. (2024). Presence of onco-fetal neighborhoods in hepatocellular carcinoma is associated with relapse and response to immunotherapy. *Nature Cancer, 5*(1), 167-186. [CrossRef]